

Design, Synthesis, and Evaluation of Novel A_{2A} Adenosine Receptor Agonists

Jayson M. Rieger,[†] Milton L. Brown,[†] Gail W. Sullivan,[‡] Joel Linden,[‡] and Timothy L. Macdonald^{*†}

Departments of Chemistry and Medicine, University of Virginia, McCormick Road, P.O. Box 400319, Charlottesville, Virginia 22904-4319

Received August 21, 2000

We have been interested in the design, synthesis, and evaluation of novel adenosine A_{2A} agonists. Through the use of comparative molecular field analysis (CoMFA) we have generated a training model that includes 78 structurally diverse A_{2A} agonists and correlated their affinity for isolated rat brain receptors with differences in their structural and electrostatic properties. We validated this model by predicting the activity of a test set that included 24 additional A_{2A} agonists. Our CoMFA model, which incorporates the physicochemical property of dipole and selects against A₁ receptor activity, generated a correlated final model ($r^2 = 0.891$) that provides for enhanced A_{2A} selectivity and predictability. Synthesis, pharmacological evaluation, and modeling of four novel ligands further validate the utility and predictive power ($r^2 = 0.626$) of the CoMFA model.

Introduction

Adenosine is an endogenous molecule that has many important biological functions and is a common substructure found in ATP, RNA, and several coenzymes.¹ It is the native ligand for adenosine receptors, also referred to as P1 purinergic receptors, which are distinct from P2 purinergic nucleotide receptors. The adenosine receptor class can be further divided into four receptor subtypes which have been identified and cloned from several mammalian tissue types: A₁, A_{2A}, A_{2B}, and A₃.² These receptors are known to elicit their biological responses through prototypical seven-transmembrane spanning G-protein coupled receptors.³ Agonists and antagonists of these receptors are being explored as potential therapeutic agents for: cardiovascular mediation,⁴ ischemia–reperfusion injury,⁵ inflammation,⁶ Parkinson's disease,⁷ and schizophrenia.⁸ We are particularly interested in the impact of adenosine A_{2A} receptor agonists on inflammation and have recently published several reports^{5,9} describing the reduction of these responses utilizing the novel ligands described here.

Because of the many potential biological implications of stimulating the various subclasses of adenosine receptors, much effort has been spent trying to elucidate SARs (structure–activity relationships) for adenosine analogues. This has led to the synthesis and evaluation of a great number of adenosine analogues.^{10–17} From this work, a general pharmacophore for A_{2A} agonists can be produced and is summarized in Chart 1. In agreement with this general pharmacophore, several ligands have evolved as standards for their specific receptor subclasses and include NECA (78), CGS21680 (113), CPA, and Cl-IB-MECA (Chart 2).

Because of the large amount of research that has been done on adenosine and its receptors, the need for models to summarize and correlate the available data is immense. Various SAR techniques have been employed to

Chart 1. General Adenosine Agonist Pharmacophore

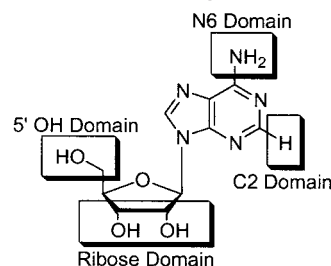
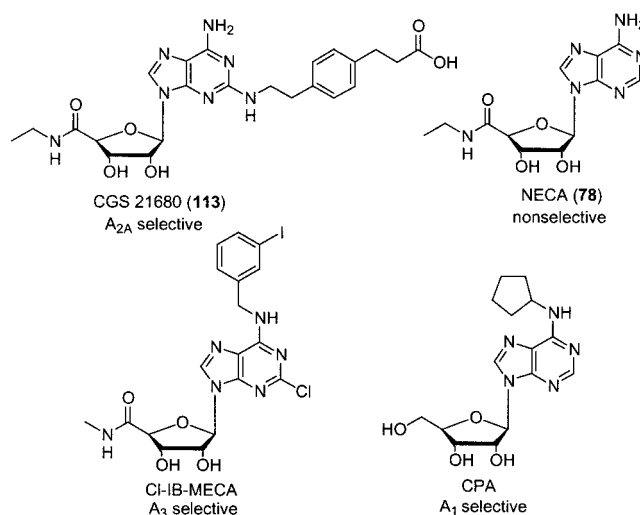


Chart 2. Several Common Selective Adenosine Receptor Agonists

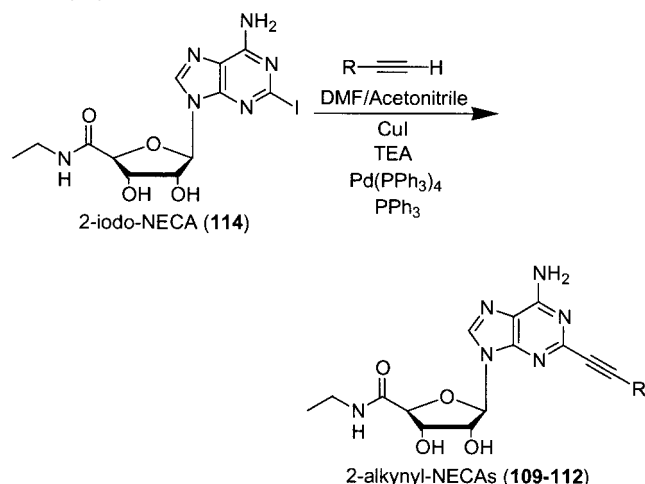


explain the observed experimental data for the ligands that have been synthesized and screened against the adenosine receptor subtypes. Recently adenosine A₁ agonists,¹⁸ adenosine A_{2A} antagonists,¹⁹ and adenosine A₃ receptor antagonists^{20–23} and agonists²⁴ have been the subject of modeling efforts. Several^{19,21,22,24} of these efforts have successfully employed the use of CoMFA (comparative molecular field analysis), which develops a predictive three-dimensional model based on differences in steric and electrostatic fields and binding

* To whom correspondence should be addressed. Phone: 804-924-7718. Fax: 804-982-2302. E-mail: tlm@virginia.edu.

[†] Department of Chemistry.

[‡] Department of Medicine.

Scheme 1. Coupling Scheme for Synthesis of Novel 2-Alkynyl-NECAs

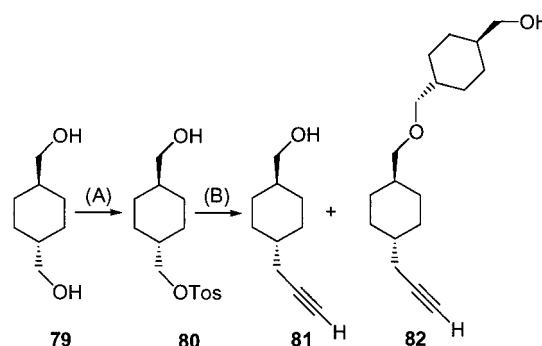
affinities. However, predictive models for adenosine A_{2A} agonists are presently lacking. Therefore, in this study we have used CoMFA to correlate a diverse group of adenosine structural modifications in order to predict a new, highly potent, and selective class of adenosine A_{2A} agonists.

Results

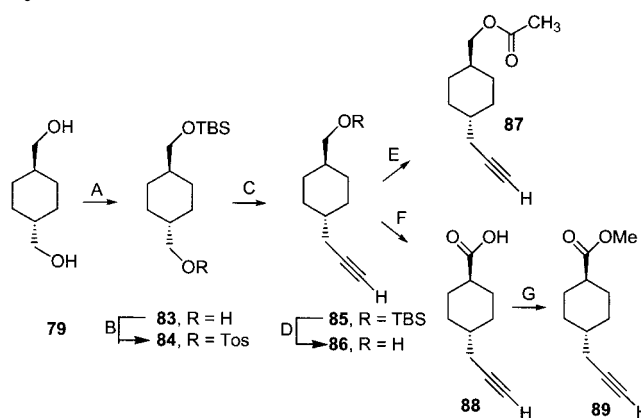
Synthesis. A plethora of substitutions have been made at the C2 position of adenosine (Chart 1) to enhance the activity and selectivity of compounds for the various receptor subclasses. Many of these substitutions are represented by compounds **1–78** which are found in Table 1. We chose to explore novel 2-alkynyl-substituted derivatives of NECA to validate our model. The novel 2-alkynyladenosines (2-AAAs) designed and evaluated in this report required the coupling of a series of terminal alkynes to 2-iodo-NECA (**114**)¹⁷ utilizing TEA and CuI in DMF/acetonitrile with catalytic $Pd(PPh_3)_4$ and PPh_3 in a classical Sonogoshira cross-coupling fashion as shown in Scheme 1. Many different attempts, including changing temperature, palladium source, and component ratio, ultimately only afforded the desired products in low to moderate yields.

The proposed compounds, **109–112**, required the synthesis of a series of novel alkynes. We envisioned the formation of these alkynes from commercially available *trans*-1,4-cyclohexanedimethanol (**79**). We first proposed formation of the desired alkynes by monotosylation, followed by insertion of the alkyne, and modification of the remaining free hydroxyl to the various proposed functionalities (carboxylic acid, methyl ester, or acetate). Unfortunately, the addition of lithium acetylide–ethylenediamine complex gave an intractable mixture of products as seen by MS and NMR believed to contain the ether **82** as shown in Scheme 2.

To circumvent this problem we utilized the synthetic protocol outlined in Scheme 3. The reaction of an excess of **79** with TBSCl (*tert*-butyl-dimethylsilyl chloride) and imidazole in DMF gave the mono-TBS alcohol. Attempts to enhance the monosilation of the diol through the use of TBSCl and NaH in THF²⁵ were unsuccessful. We then introduced the tosyl group to **83** under typical conditions,²⁶ preparing the molecule for introduction of the acetylene moiety and formation of **84**.

Scheme 2. First Synthetic Route Toward Ligand Synthesis^a

^a Reaction conditions: (A) (i) NaH, THF, (ii) TosCl; (B) lithium acetylide ethylenediamine complex, DMSO.

Scheme 3. Final Synthetic Route Toward Ligand Synthesis^a

^a Reaction conditions: (A) TBSCl, imidazole, DMF; (B) TosCl, pyridine; (C) lithium acetylide, DMSO; (D) TBAF, THF; (E) acetic anhydride, pyridine, THF; (F) Jones oxidation; (G) TMS–diazomethane, MeOH/ $CHCl_3$.

Introduction of the terminal acetylene was accomplished through the in situ formation of lithium acetylide²⁷ by bubbling acetylene gas into a solution of lithium wire in liquid ammonia. After addition of DMSO, the ammonia was removed and tosylate **84** was added ultimately affording compound **85**. Interestingly, some deprotected alcohol **86** (approximately 10–20%) was also observed upon working up the reaction. In an effort to increase the overall yield, the crude mixture was treated with TBAF hydrate, generating **86** in an overall yield of 93% through both steps. This alkyne was either coupled to 2-iodo-NECA (**114**) directly or converted to a carboxylic acid, acetate, or methyl ester. Treating **86** with acetic anhydride and pyridine gave the acetate **87**. Jones oxidation of **86** gave the carboxylic acid **88**, and the methyl ester **89** was formed by treating **88** with TMS–diazomethane. These compounds, **86–89**, were coupled with 2-iodo-NECA to form the novel A_{2A} agonists ATL2037 (**112**), ATL193 (**111**), ATL146a (**109**), and ATL146e (**110**), respectively.

Pharmacology. The four novel compounds synthesized in this report were evaluated by competitive binding assays employing the A_{2A} receptors in rat striatal membranes ($[^{125}I]APE$)²⁸ or A_1 receptors of rat cortex ($[^{125}I]ABA$).²⁹ Compounds **109–112** were potent agonists, ranging in binding affinities from $K_i = 20$ nM to 0.5 nM at the A_{2A} receptor (see Table 2). They also

Table 1. Structures and Biological Data for Compounds in the Training Set

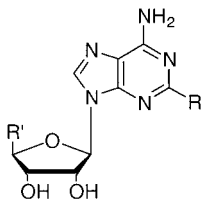
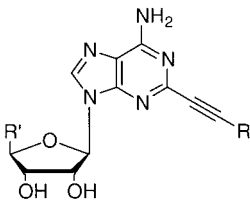
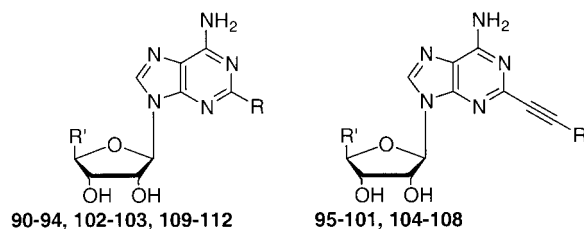
									
		1-36, 68-78		37-67					
compd	R	NECA* (R')	A ₁ (nM)	A _{2A} (nM)	log(norm A ₁)	−log(norm A _{2A})	dipole	energy (kcal)	
1	2-ethyl-1-butoxy	N	2700 ^a	4600 ^a	−5.276	5.324	1.66	46.235	
2	3-ethyl-1-pentoxy	N	1490 ^a	530 ^a	−5.534	6.262	1.71	47.865	
3	3-pentyl-1-oxy	N	460 ^a	150 ^a	−6.045	6.811	1.73	45.431	
4	cyclopentylloxy	N	14000 ^a	1000 ^a	−4.561	5.987	3.45	52.200	
5	cyclohexylmethoxy	N	3000 ^a	3200 ^a	−5.230	5.482	1.89	42.335	
6	2-cyclopentylethoxy	N	1600 ^a	120 ^a	−5.503	6.908	1.65	53.581	
7	2-cyclohexylethoxy	N	1600 ^a	22 ^a	−5.503	7.644	2.02	43.426	
8	3-cyclohexyl-1-propoxy	N	2800 ^a	22 ^a	−5.260	7.644	1.85	43.700	
9	4-cyclohexyl-1-butoxy	N	1100 ^a	18 ^a	−5.666	7.731	1.90	44.163	
10	phenoxy	N	3500 ^a	5700 ^a	−5.163	5.231	1.57	43.570	
11	benzyloxy	N	600 ^a	2200 ^a	−5.929	5.644	1.64	42.908	
12	2-phenylethoxy	N	130 ^a	17 ^a	−6.594	7.756	1.74	42.488	
13	Cl	N	6.7 ^a	76 ^a	−7.881	7.106	2.46	40.942	
14	ethoxy	N	1300 ^a	1500 ^a	−5.594	5.811	1.83	41.882	
15	3-phenyl-1-propoxy	N	3600 ^a	1200 ^a	−5.151	5.908	1.58	42.636	
16	4-phenyl-1-butoxy	N	2400 ^a	170 ^a	−5.327	6.756	1.64	42.445	
17	5-phenyl-1-pentoxy	N	960 ^a	53 ^a	−5.725	7.262	1.59	43.000	
18	(2 <i>S</i>)-phenyl-1-butoxy	N	2300 ^a	430 ^a	−5.346	6.353	1.95	42.237	
19	(3 <i>S</i>)-phenyl-1-butoxy	N	1600 ^a	1700 ^a	−5.503	5.756	1.78	42.627	
20	2-(2-chlorophenyl)ethoxy	N	520 ^a	56 ^a	−5.992	7.239	1.24	42.181	
21	2-(3-chlorophenyl)ethoxy	N	250 ^a	76 ^a	−6.310	7.106	0.84	42.033	
22	2-(4-chlorophenyl)ethoxy	N	89 ^a	22 ^a	−6.758	7.644	2.13	42.060	
23	2-hydroxyethoxy	N	72 ^a	690 ^a	−6.850	6.148	1.98	42.311	
24	2-(3-fluorophenyl)ethoxy	N	150 ^a	58 ^a	−6.531	7.223	0.85	42.194	
25	2-(4-fluorophenyl)ethoxy	N	500 ^a	97 ^a	−6.009	7	2.16	42.202	
26	2-(2-methylphenyl)ethoxy	N	450 ^a	39 ^a	−6.054	7.396	2.01	43.492	
27	2-(3-methylphenyl)ethoxy	N	140 ^a	61 ^a	−6.561	7.201	2.04	42.741	
28	2-(4-methylphenyl)ethoxy	N	49 ^a	11 ^a	−7.017	7.945	1.85	42.758	
29	2-(2-methoxyphenyl)ethoxy	N	190 ^a	36 ^a	−6.429	7.430	1.80	44.000	
30	2-(4-methoxyphenyl)ethoxy	N	480 ^a	32 ^a	−6.026	7.482	1.47	44.191	
31	2-(3,4-dimethoxyphenyl)ethoxy	N	380 ^a	40 ^a	−6.128	7.385	2.07	45.561	
32	1-propoxy	N	1200 ^a	360 ^a	−5.628	6.430	1.78	42.040	
33	2-(3,4,5-dimethoxyphenyl)ethoxy	N	5000 ^a	330 ^a	−5.009	6.468	1.71	46.848	
34	1-butoxy	N	2500 ^a	270 ^a	−5.310	6.555	1.79	42.223	
35	1-hexyloxy	N	890 ^a	160 ^a	−5.758	6.783	1.78	42.594	
36	2-methyl-1-propoxy	N	2600 ^a	700 ^a	−5.293	6.142	1.68	41.894	
37	<i>p</i> -PhNH ₂	Y	599 ^b	113 ^b	−6.240	6.839	2.55	37.774	
38	<i>p</i> -PhCF ₃	Y	2432 ^b	315 ^b	−5.631	6.394	3.37	37.792	
39	<i>p</i> -PhF	Y	3312 ^b	81.4 ^b	−5.497	6.981	2.55	37.665	
40	<i>p</i> -PhCONH ₂	Y	7498 ^b	1500 ^b	−5.142	5.716	2.18	40.192	
41	<i>o</i> -PhCHO	Y	6864 ^b	1158 ^b	−5.180	5.828	0.90	37.584	
42	<i>m</i> -PhCHO	Y	1435 ^b	176 ^b	−5.860	6.647	2.46	37.736	
43	<i>p</i> -PhNO ₂	Y	900 ^b	21.5 ^b	−6.063	7.560	6.34	39.991	
44	<i>p</i> -Ph(CH ₂)COOtBu	Y	ND	743 ^b	ND	6.021	2.95	38.331	
45	1-naphthyl	Y	4463 ^b	488 ^b	−5.367	6.204	2.33	38.696	
46	(CH ₂) ₃ Ph	Y	209 ^b	1.2 ^b	−6.697	8.813	2.93	38.479	
47	3-pyridyl	Y	139 ^b	234 ^b	−6.874	6.523	3.00	37.971	
48	4-pyridyl	Y	428 ^b	87 ^b	−6.386	6.953	2.40	37.930	
49	2-furyl	Y	310 ^b	130 ^b	−6.526	6.778	2.27	46.536	
50	2-thienyl	Y	597 ^b	19.5 ^b	−6.241	7.602	3.15	40.539	
51	2-thiazolyl	Y	85.4 ^b	41.3 ^b	−7.086	7.276	3.63	43.980	
52	CH ₂ - <i>N</i> -imidazolyl	Y	178 ^b	16.5 ^b	−6.767	7.675	4.86	61.210	
53	CH ₂ - <i>N</i> -morpholinyl	Y	90.5 ^b	27.4 ^b	−7.060	7.454	3.74	43.955	
54	Ph	Y	698 ^b	120 ^b	−6.173	6.813	2.50	37.953	
55	<i>p</i> -PhOH	Y	497 ^b	20.6 ^b	−6.321	7.578	2.74	38.717	
56	(CH ₂) ₃ CH ₃	Y	130 ^b	2.2 ^b	−6.903	8.550	2.50	38.031	
57	NH(CH ₂) ₂ Ph	Y	473 ^c	9.7 ^c	−6.089	8.081	2.50	39.019	
58	NHCH ₂ Ph	Y	8604 ^c	1130 ^c	−4.829	6.015	2.24	39.005	
59	NH(CH ₂) ₂ (4-fluorophenyl)	Y	1184 ^c	7.7 ^c	−5.690	8.182	3.42	38.732	
60	N(CH ₃)((CH ₂) ₂ Ph)	Y	12100 ^c	71 ^c	−4.681	7.217	2.88	39.558	
61	NH(CH ₂) ₂ (4-(CH ₂ COOH)phenyl)	Y	4880 ^c	45 ^c	−5.075	7.415	2.78	40.618	
62	NH(CH ₂) ₂ (4-(CH ₂ COOMe)phenyl)	Y	1257 ^c	9 ^c	−5.664	8.114	3.62	40.593	
63	<i>c</i> -C ₆ H ₉	N	88 ^d	12 ^d	−7.067	7.732	2.39	51.132	
64	<i>c</i> -C ₆ H ₁₁	N	138 ^d	10 ^d	−6.872	7.811	2.41	41.041	
65	<i>c</i> -C ₆ H ₁₁ (CH ₂) ₂	N	313 ^d	26 ^d	−6.516	7.396	2.25	42.299	
66	Ph	N	701 ^d	109 ^d	−6.166	6.774	2.45	41.240	

Table 1. (Continued)

compd	R	NECA* (R')	A ₁ (nM)	A _{2A} (nM)	log(norm A ₁)	−log(norm A _{2A})	dipole	energy (kcal)
67	Ph(CH ₂) ₂	N	400 ^d	37 ^d	−6.409	7.243	2.22	40.377
68	CH ₂ CH ₃	N	186 ^e	21.2 ^e	−6.854	7.767	2.35	40.601
69	(CH ₂) ₂ CH ₃	N	154 ^e	7.5 ^e	−6.936	8.218	2.29	40.698
70	(CH ₂) ₃ CH ₃	N	126 ^e	2.8 ^e	−7.023	8.646	2.29	40.869
71	(CH ₂) ₅ CH ₃	N	202 ^e	12.1 ^e	−6.819	8.011	2.22	41.205
72	CH ₂ OH	N	10.1 ^e	20.5 ^e	−8.120	7.782	3.41	40.923
73	(CH ₂) ₂ OH	N	81.4 ^e	40.1 ^e	−7.213	7.490	2.64	40.963
74	CH ₂ OCH ₃	N	38.1 ^e	88.1 ^e	−7.543	7.148	2.85	41.213
75	CH ₂ O(CH ₂) ₂ CH ₃	N	18.5 ^e	10.6 ^e	−7.857	8.068	2.72	41.741
76	(CH ₂) ₂ O(CH ₂) ₂ CH ₃	N	128 ^e	10.2 ^e	−7.017	8.085	2.22	41.420
77	(CH ₂) ₃ OCH ₂ CH ₃	N	244 ^e	12.8 ^e	−6.736	7.986	2.65	41.466
78 (NECA)	H		13.3 ^e	12.4 ^e	−8.000	8.000	2.61	40.318

*Y refers to R' = NECA modification (N-ethylcarboxamide); N refers to R' = CH₂OH. ^a Reported in ref 11. ^b Reported in ref 10. ^c Reported in ref 15. ^d Reported in ref 12. ^e Reported in ref 16. Normalized data found by multiplying or dividing the respective paper's IC₅₀ value for NECA by a factor that converts NECA to a standard value of 10 nM for both A₁ and A_{2A} assays. ND = no data available.

Table 2. Structures and Biological Data for Compounds in the Test Set

compd	R	NECA* (R')	A ₁ (nM)	A _{2A} (nM)	log(norm A ₁)	−log(norm A _{2A})	dipole	energy (kcal)
90	2-(4-methyl-1-pentoxy)	N	2100 ^a	130 ^a	−5.39	6.87	1.90	43.200
91	Cl	N	6.7 ^a	76 ^a	−7.88	7.11	2.46	40.942
92	2-[2-(3-fluorophenyl)ethoxy]	N	180 ^a	110 ^a	−6.45	6.95	1.28	42.121
93	2-[2-(3-methoxyphenyl)ethoxy]	N	760 ^a	320 ^a	−5.83	6.48	1.23	44.106
94	2-(2-propoxy)	N	20000 ^a	7400 ^a	−4.41	5.12	1.19	41.924
95	CH ₂ Ph	Y	27.4 ^b	1.6 ^b	−7.58	8.67	2.63	38.655
96	2-pyridyl	Y	114 ^b	89.8 ^b	−6.96	6.94	2.63	38.229
97	2-thiazolyl	Y	85.4 ^b	41.3 ^b	−7.09	7.28	1.10	44.029
98	CH ₂ -N-imadazolyl	Y	178 ^b	16.5 ^b	−6.78	7.68	5.03	61.243
99	<i>p</i> -PhCH ₃	Y	500 ^b	36.3 ^b	−6.32	7.33	5.03	38.203
100	<i>p</i> -PhCH ₂ CN	Y	1603 ^b	54.8 ^b	−5.81	7.15	3.11	37.629
101	<i>p</i> -PhOCH ₃	Y	414 ^b	52.4 ^b	−6.40	7.17	2.43	39.567
102	<i>p</i> -ClC ₆ H ₄ (CH ₂) ₂ NH	Y	1505 ^c	7.5 ^c	−5.59	8.19	3.38	38.586
103	<i>p</i> -(HOOCCH ₂ O)C ₆ H ₄ (CH ₂) ₂ NH	Y	4250 ^c	42 ^c	−5.14	7.45	4.87	41.875
104	<i>c</i> -C ₅ H ₉ CH ₂	N	162 ^d	2.3 ^d	−6.80	8.45	2.61	50.941
105	<i>c</i> -C ₅ H ₉ (CH ₂) ₂	N	136 ^d	3.4 ^d	−6.88	8.28	2.25	51.167
106	<i>c</i> -C ₆ H ₁₁ CH ₂	N	208 ^d	6.5 ^d	−6.69	8.00	2.48	41.102
107	(CH ₂) ₄ CH ₃	N	170 ^e	5.4 ^e	−6.89	8.36	2.25	41.019
108	H	N	272 ^e	37.6 ^e	−6.69	7.52	2.23	40.701
109	4-(COOH)C ₆ H ₁₀ CH ₂	Y	292	20.1	−5.50	7.23	1.02	40.559
110	4-(COOCH ₃)C ₆ H ₁₀ CH ₂	Y	28.1	4.5	−6.54	7.88	1.90	44.449
111	4-(CH ₂ OAc)C ₆ H ₁₀ CH ₂	Y	14.0	6.2	−6.82	7.74	2.80	42.512
112	4-(CH ₂ OH)C ₆ H ₁₀ CH ₂	Y	0.84	0.48	−8.04	8.85	2.33	38.740
113	NA	NA	1800 ^a	19 ^a	−5.45	7.71	4.02	39.973

*Y refers to R' = NECA modification (N-ethylcarboxamide); N refers to R' = CH₂OH. ^a Reported in ref 11. ^b Reported in ref 10. ^c Reported in ref 15. ^d Reported in ref 12. ^e Reported in ref 16. Normalized data found by multiplying or dividing the respective paper's IC₅₀ value for NECA by a factor that converts NECA to a standard value of 10 nM for both A₁ and A_{2A} assays. NA = not available.

demonstrated moderate selectivity against the A₁ receptor, with nearly 2–15-fold differences in binding affinity favoring the A_{2A} receptor. These compounds all incorporate key SAR features known to contribute to high A_{2A} affinity and selectivity: namely an aliphatic alkyne with a polar terminal group at C2 and an ethylcarboxamide group at the 5' position.

Molecular Modeling. CoMFA was employed as a tool for elucidating the structural and electrostatic requirements for high-affinity A_{2A} receptor binding. Using previously reported A_{2A} agonists that also had available A₁ receptor data, we compiled the representative list of compounds found in Tables 1 and 2. We designed our CoMFA model both to be selective for

potent A_{2A} activity and to minimize activity at the A₁ receptor subtype. We hypothesized that this would provide us with a more useful and global model that was predictive for both potency at A_{2A} and selectivity over A₁. Furthermore, traditional QSAR observations indicated that several of the more potent compounds contained terminal polar functionalities. This led us to explore the use of molecular dipole moment as an additional physical descriptor.

To generate the models we first obtained the X-ray crystal structure for adenosine³⁰ (Cambridge ref code = ADENOS01) and NECA³¹ (Cambridge ref code = KEMYEG). Through the use of the AGGREGATE function within SYBYL, we fixed these low-energy confor-

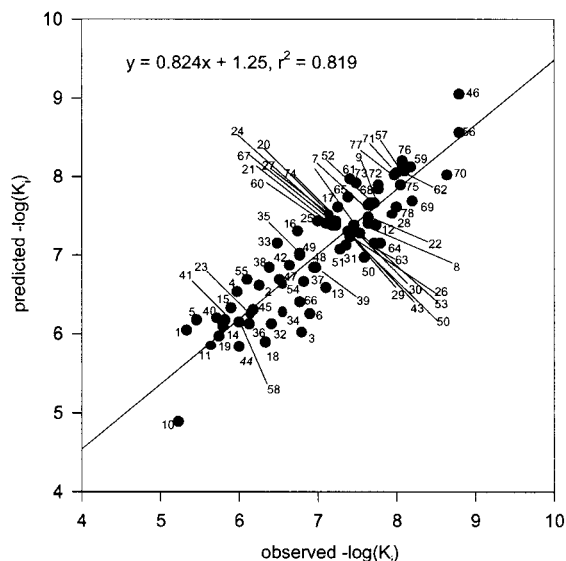


Figure 1. Plot of final non-cross-validated observed versus predicted for A_{2A} model with no independent variables for the training set.

mations and subsequently added the C2 substitutions described in Tables 1 and 2. All compounds were aligned through the root-mean-square (rms) fit of N3, C6, N7, and N9 of their respective purine rings. Before performing partial-least-squares (PLS) analysis on the compounds, it was necessary to normalize the K_i values because they were obtained from multiple sources. For consistency, NECA was assigned a K_i of 10 nM and all compounds were adjusted appropriately. To allow for selectivity, A_{2A} values were incorporated into the molecular spreadsheet as $-\log(K_i)$, whereas A₁ data was incorporated as $\log(K_i)$. This approach represents a mathematically valid and useful method for generating receptor subtype-selective CoMFA models. In this method the displayed CoMFA fields represent potential modifications/substitutions requisite to enhance A_{2A} potency and selectivity over A₁ receptors simultaneously.

After molecular alignment, PLS analysis with cross-validation led to the optimum number of components (4, 4, 5, 6) and r^2_{cv} (0.622, 0.541, 0.653, 0.646) for the A₁, A_{2A}, A₁/A_{2A}, and A₁/A_{2A}/dipole models, respectively. For the latter two models that included additional descriptors (A₁ data and molecular dipole), those values were incorporated as additional independent variables along with the CoMFA value, while A_{2A} was maintained as the dependent variable. Using the optimum number of components, non-cross-validated PLS analysis was performed and resulted in r^2 values of 0.877, 0.817, 0.863, and 0.890, respectively. Through the addition of A₁ receptor binding and molecular dipole moment, the r^2 for the A_{2A} model increases by 0.073 and the standard error of estimate decreased by nearly 0.1 log unit. This data is graphically represented in Figures 1 and 2.

The most important part of validating a model is the evaluation of that model for accuracy in predicting the test set. The test set clearly indicates that the A₁/A_{2A}/dipole model has far greater predictive powers ($r^2 = 0.626$) in comparison to the model of only A_{2A} data ($r^2 = 0.438$). Furthermore, the model predicts high binding affinity for the four novel compounds synthesized, **109–112**, which is confirmed by the experimental binding values. This data is summarized in Figures 3 and 4.

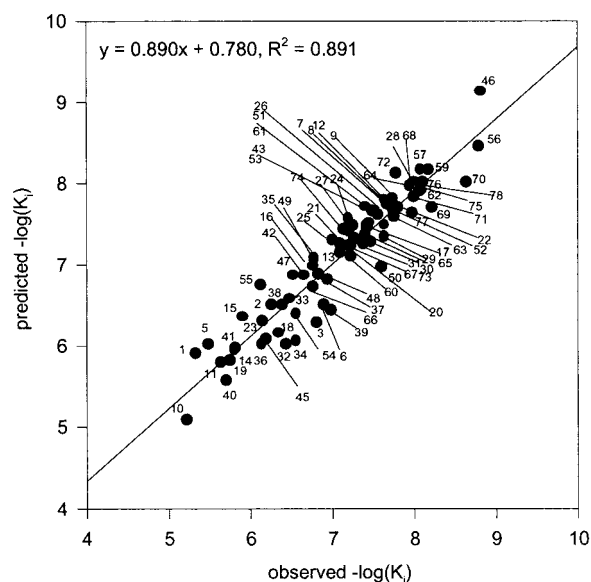


Figure 2. Plot of final non-cross-validated observed versus predicted for A_{2A} model with A₁ and dipole as independent variables for the training set.

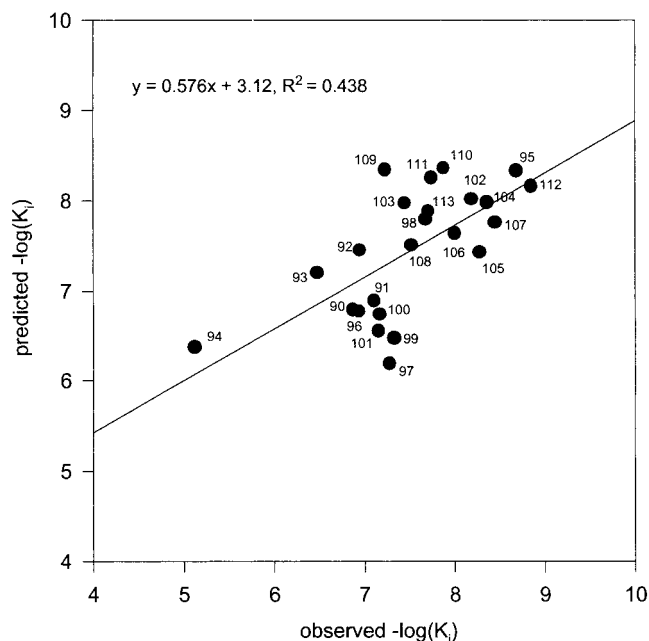


Figure 3. Plot of final non-cross-validated observed versus predicted for A_{2A} model with no independent variables for the test set.

The difference in predictive powers of the model that includes A₁ values as well as molecular dipole moment is also apparent when viewing the CoMFA contour maps that are generated, as seen in Figures 5 and 6. There is a noticeable increase in the amount of sterically restricted space as indicated by the larger yellow fields as well as the new presence of sterically and electrostatically favorable fields near the 5' position of the adenosine backbone.

Discussion and Conclusions

We have successfully generated a CoMFA model ($r^2 = 0.890$) based on 78 structurally diverse C2-modified adenosine derivatives. Our model, which is predictive for A_{2A} activity, also allows for selectivity against the

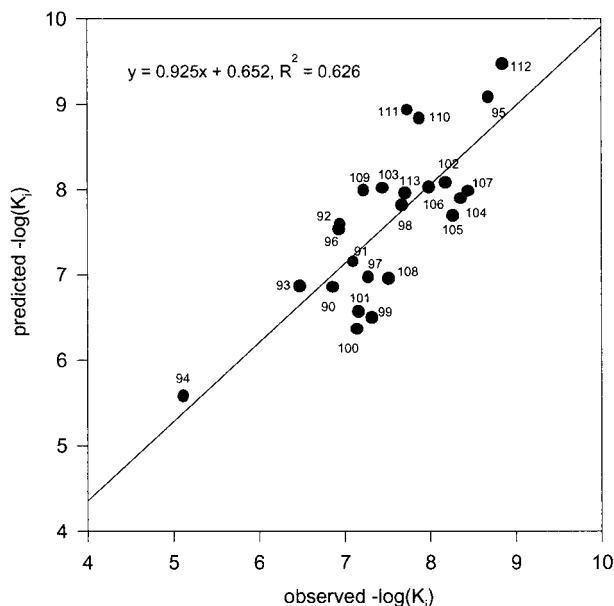


Figure 4. Plot of final non-cross-validated observed versus predicted for A_{2A} model with A_1 and dipole as independent variables for the test set.

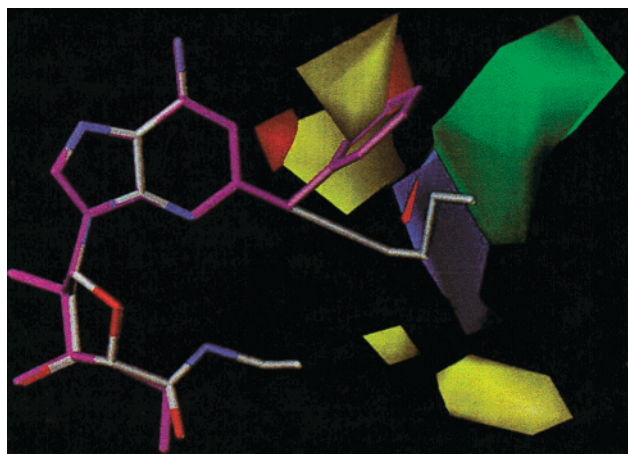


Figure 5. Steric and electrostatic CoMFA contour maps for A_{2A} model with no independent variables with compounds **10** (pink) and **70** (gray).

A_1 receptor subtype through incorporation of A_1 K_i values as an additional independent variable. This represents the first A_{2A} adenosine receptor CoMFA model that also incorporates a selectivity factor against A_1 binding as well as the first CoMFA model for adenosine A_{2A} agonists. Furthermore, we found that the molecular dipole moment is a useful physical descriptor that enhances the models predictive ability. We have used this model to predict the A_{2A} rat striatum K_i values for an additional 24 compounds not found in the training set. While the model that includes A_1 K_i values and molecular dipole moment led to only a modest difference in r^2 for the training set, a pronounced enhancement was apparent for the test set ($r^2 = 0.626$ vs $r^2 = 0.438$).

Our model also very accurately distinguishes between ortho-, meta-, and para-substituted phenyl derivatives **20–22**, **24–31**, and **37–43** as well as a large diversity of functionalized and nonfunctionalized hydrocarbons. In comparing the CoMFA contour plots for the two models, the impact of the A_1 data is readily apparent in the larger yellow field directly adjacent to the C2

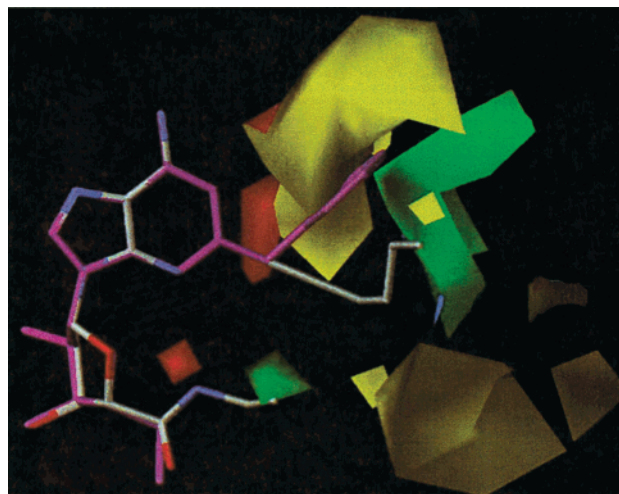


Figure 6. Steric and electrostatic CoMFA contour maps for A_{2A} model with A_1 and dipole as independent variables with compounds **10** (pink) and **70** (gray).

carbon of the purine ring indicating decreased activity with compounds that explore that area of space. This supports the hypothesis that there is a narrow pocket that opens up to a much larger binding region with which many of the C2-substituted compounds interact. Thus, while compounds with short linkers have poorer A_{2A} activity, they are generally more A_1 -active. The model also appears to strongly suggest that the NECA modification does indeed make a contribution to the potency/selectivity of A_{2A} agonists. This is evident from the new CoMFA contour fields generated near the adenosine 5' region in the A_1/A_{2A} /dipole model.

To further validate our model we also embarked on the synthesis and evaluation of four compounds, **109–112**, from a novel structural class. Our experimentally determined normalized A_{2A} binding values (59, 13, 18, and 1.4 nM, respectively) correlate quite well with our predicted values (10, 1.5, 1.2, and 0.34 nM, respectively) from our CoMFA model. Thus, our model will continue to be quite useful in our quest to design additional potent and selective A_{2A} agonists. We plan to continue this work through the examination of the functional utility of these compounds as mediators of ischemia–reperfusion injury and inflammation. We are also currently examining these compounds in cloned human receptors to examine species differences and will report on these results shortly.

Experimental Section

All melting points were determined with a Thomas-Hoover capillary melting point apparatus and are uncorrected. Nuclear magnetic resonance spectra for proton (^1H NMR) were recorded on a 300-MHz GE spectrophotometer. The chemical shift values are expressed in ppm (parts per million) relative to tetramethylsilane. For data reporting: s = singlet, d = doublet, t = triplet, q = quartet, and m = multiplet. Mass spectra were measured on a Finnigan LcQ Classic. High-resolution mass spectrometry (HRMS) data was provided by the Nebraska Center for Mass Spectrometry. Analytical HPLC was done on a Waters 2690 separation module with a Waters symmetry C8 (2.1×150 mm) column operated at room temperature. Compounds were eluted at 200 $\mu\text{L}/\text{min}$ with 70:30 acetonitrile/water, containing 0.5% acetic acid, with UV detection at 214 nm using a Waters 486 tunable detector. Preparative HPLC was performed on a Shimadzu Discovery HPLC with a Shim-pack VP-ODS C18 (20×100 mm) column operated at room

temperature. Compounds were eluted at 30 mL/min with a gradient 20–80% of water (containing 0.1% TFA) to methanol over 15 min with UV detection at 214 nm using a SPD10A VP tunable detector. All final compounds presented here were determined to be greater than 98% pure by HPLC. Flash chromatography was performed on silica 60A gel (230–400 mesh) using the method of Still.³² Analytical thin-layer chromatography was done on Merck Kieselgel 60 F254 aluminum sheets. All reactions were done under a nitrogen atmosphere in flame-dried glassware unless otherwise stated.

[4-(*tert*-Butyldimethylsilyloxyethyl)cyclohexyl]-methanol (83**).** To a 100-mL flask containing **79** (4.0 g, 27.8 mmol) in DMF (40 mL) were added TBDMSCl (3.56 g, 23.6 mmol) and imidazole (3.79 g, 55.6 mmol). The reaction was allowed to stir at 25 °C for 16 h after which time saturated aqueous LiBr (50 mL) was added and the reaction extracted with ether (2 × 50 mL). The ether layers were pooled and extracted again with LiBr (2 × 35 mL) resulting in the ether layer becoming a clear solution. The ether layer was then concentrated in vacuo and flash chromatographed on a silica gel column eluting with 1:2 ether/petroleum ether to yield **83** (3.80 g, 62%) as a homogeneous oil: ¹H NMR (CDCl₃) δ 3.46 (d, *J* = 6.2 Hz, 2 H), 3.39 (d, *J* = 6.2 Hz, 2 H), 1.95–1.72 (m, 4 H), 1.65 (m, 1 H), 1.40 (m, 1 H), 1.03–0.89 (m, 4 H), 0.88 (s, 9 H), 0.04 (s, 6 H); ¹³C NMR (CDCl₃) δ 69.2, 69.1, 41.2, 41.1, 29.5, 26.5, 18.9, –4.8; APCI *m/z* (rel intensity) 259 (MH⁺, 100).

Toluene-4-sulfonic Acid 4-(*tert*-Butyldimethylsilyloxyethyl)cyclohexylmethyl Ester (84**).** To a 100-mL flask containing **83** (3.4 g, 13.2 mmol) in CHCl₃ (30 mL) were added tosyl chloride (3.26 g, 17.1 mmol) and pyridine (3.2 mL, 39.6 mmol). The reaction was allowed to stir at 25 °C for 14 h after which time the reaction was concentrated in vacuo to yield a wet white solid. To this solid was added ether (50 mL) and the solid was filtered and subsequently washed with additional ether (2 × 50 mL). The ether layers were pooled, concentrated in vacuo to yield a clear oil which was flash chromatographed on a silica gel column eluting with 1:4 ether/petroleum ether to yield **84** (4.5 g, 83%) as a white solid: ¹H NMR (CDCl₃) δ 7.78 (d, *J* = 7.7, 2 H), 7.33 (d, *J* = 7.7 Hz, 2 H), 3.81 (d, *J* = 6.2 Hz, 2H), 3.37 (d, *J* = 6.2, 2 H), 2.44 (s, 3 H), 1.95–1.72 (m, 4 H), 1.65 (m, 1 H), 1.40 (m, 1 H), 1.03–0.89 (m, 4 H), 0.88 (s, 9 H), 0.04 (s, 6 H); ¹³C NMR (CDCl₃) δ 145.1, 133.7, 130.3, 128.4, 75.8, 68.9, 40.7, 38.0, 29.1, 26.5, 22.1, 18.9, –4.9; APCI *m/z* (rel intensity) 413 (MH⁺, 100).

(4-Prop-2-ynylcyclohexyl)methanol (86**).** A three-neck 250-mL flask equipped with a gas inlet tube and dry ice condenser was cooled to –78 °C and charged with liquid ammonia (40 mL). To the reaction mixture was added lithium wire (600 mg, 86.4 mmol) generating a deep blue solution. Subsequently, the mixture was allowed to stir for 1 h. Acetylene, that was passed through a charcoal drying tube, was added to the ammonia until all the lithium had reacted and the solution turned colorless, at which time the flow of acetylene was stopped, the acetylene-inlet tube and condenser removed and the flask outfitted with a thermometer. DMSO (20 mL) was added and the ammonia evaporated with a warm water bath until the mixture reached a temperature of 30 °C and stirred at this temperature for 2 h until the solution stopped bubbling. The mixture was then cooled to 5 °C and **84** (11.25 g, 27.3 mmol) was added dissolved in DMSO (10 mL) while maintaining the temperature at 5 °C. The mixture was allowed to stir at 5 °C for 0.5 h and then gradually warmed to room temperature and stirred for an additional 18 h. The brown/black reaction mixture was poured slowly over ice (300 g) and extracted with ether (4 × 100 mL), dried with anhydrous sodium sulfate, and concentrated in vacuo to yield a yellow oil. The oil was subsequently dissolved in THF (200 mL) and changed to a brownish color upon addition of TBAF hydrate (11.20 g, 35.5 mmol). The solution was allowed to stir for 24 h under N₂ atmosphere, after which time it was quenched with water (200 mL) and extracted with ether (3 × 100 mL). The ether was then concentrated in vacuo and chromatographed on a silica gel column eluting with 1:1 ether/petroleum ether to yield **86** (3.91 g, 93%) as a yellow oil: ¹H NMR (CDCl₃)

δ 3.45 (d, *J* = 6.2, 2 H), 2.10 (d, *J* = 6.2, 2 H), 1.9 (s, 1 H), 1.94–1.69 (m, 4 H), 1.52–1.34 (m, 2 H), 1.16–0.83 (m, 4 H); ¹³C NMR (CDCl₃) δ 83.8, 69.5, 69.0, 40.8, 37.7, 32.3, 29.7, 26.5.

(4-Prop-2-ynylcyclohexyl)methyl Acetate (87**).** To a solution of **86** (6.31 mmol) in 6 mL DMF were added 0.62 mL (7.57 mmol) pyridine and 0.78 mL (8.27 mmol) acetic anhydride. The reaction was allowed to stir overnight at room temperature. After 16 h some starting material still remained. The reaction was then heated at 75 °C for 3 h. The solvent was then removed under reduced pressure to yield a yellow oil which was purified by flash chromatography on silica gel eluting with 1:3 ether/petroleum ether to yield 1.12 g (91%) of **87** as an oil: ¹H NMR (CDCl₃) δ 3.87 (d, *J* = 6.2 Hz, 2 H), 2.06 (d, *J* = 4.3 Hz, 2 H), 2.03 (s, 3 H), 1.98–1.93 (m, 1 H), 1.92–1.83 (m, 2 H), 1.83–1.74 (m, 2 H), 1.63–1.36 (m, 2 H), 1.12–0.90 (m, 4 H); ¹³C NMR (CDCl₃) δ 171.7, 83.7, 69.9, 69.6, 37.4, 37.3, 32.1, 29.7, 26.5, 21.4; APCI *m/z* (rel intensity) 195 (M⁺, 30), 153 (M⁺, 70), 135 (M⁺, 100).

4-Prop-2-ynylcyclohexanecarboxylic Acid (88**).** A solution of chromium trioxide (600 mg, 6.0 mmol) in 1.5 M H₂SO₄ (2.6 mL, 150 mmol) was cooled to 5 °C and added to a solution of **86** (280 mg, 1.84 mmol) in acetone (15 mL). The mixture was allowed to warm to room temperature and allowed to stir overnight. 2-Propanol (4 mL) was added to the green/black solution, which turned light blue after 1 h. After adding water (15 mL), the solution was extracted with CHCl₃ (6 × 25 mL). The organics were pooled and concentrated in vacuo to yield a white solid. The solid was dissolved in ether (50 mL) and extracted with 1 M NaOH (2 × 30 mL). The basic extracts were pooled, acidified with 10% HCl, and re-extracted with ether (3 × 30 mL). The ether layers were then dried with sodium sulfate and concentrated in vacuo to yield a white solid which was recrystallized from acetone/water to yield **88** (222 mg, 73%) as white needles: mp 84–85 °C; ¹H NMR (CDCl₃) δ 2.30–2.23 (m, 1 H), 2.17–2.11 (m, 2 H), 2.07–2.03 (m, 2 H), 1.97–1.91 (m, 3H), 1.51–1.39 (m, 3 H), 1.13–1.01 (m, 2 H); ¹³C NMR (CDCl₃) δ 182.5, 83.8, 69.6, 40.7, 37.7, 32.3, 29.6, 26.5; APCI *m/z* (rel intensity) 165 (M⁺, 100).

Methyl 4-Prop-2-ynylcyclohexanecarboxylate (89**).** To a solution of **88** (240 mg, 1.45 mmol) in 7:3 CH₂Cl₂/MeOH (10 mL) was added TMS-diazomethane (2.0 M in hexanes) (0.9 mL, 1.8 mmol) in 0.2-mL aliquots until the color remained yellow. The reaction was allowed to stir for an additional 0.25 h at room temperature after which time glacial acetic acid was added dropwise until the solution became colorless. The reaction was then concentrated in vacuo to an oil which was purified by flash chromatography on silica gel using ether/petroleum ether (1:9) to yield **89** (210 mg, 80%) as a clear oil: ¹H NMR (CDCl₃) δ 3.60 (s, 3H), 2.25–2.13 (m, 1 H), 2.08–1.94 (m, 3 H), 1.95–1.90 (m, 2 H), 1.49–1.31 (m, 3 H), 1.10–0.93 (m, 2 H); ¹³C NMR (CDCl₃) δ 176.7, 83.3, 69.8, 51.9, 43.4, 36.7, 31.9, 29.2, 26.3; APCI *m/z* (rel intensity) 181 (MH⁺, 100).

General Method for the Preparation of 2-AAs 109–112. To a solution of 2-iodo-NECA (0.025 mmol) and terminal alkyne (0.045 mmol) in DMF/acetonitrile (0.5 mL/1 mL) were added TEA (0.76 mmol), Pd(PPh₃)₄ (0.0038 mmol), CuI (0.0046 mmol), and PPh₃ (0.0038 mmol). The clear yellow solution was heated to 60 °C for 12 h under a nitrogen atmosphere to yield a brown/black solution. After the starting material was completely consumed, as judged by TLC (CHCl₃/MeOH 4:1), the solvent was removed in vacuo to yield a syrup that was purified via silica gel column chromatography using 6% MeOH/CHCl₃ to yield pure products.

4-[3-[6-Amino-9-(5-ethylcarbamoyl)-3,4-dihydroxytetrahydrofuran-2-yl]-9H-purin-2-yl]prop-2-ynylcyclohexanecarboxylic Acid (109**).** The reaction of **110** with 5 equiv of LiOH in THF/water for 6 h gave **109** (7 mg, 72%) as a white solid which was crystallized from MeOH/H₂O (0.1% TFA) after purification by reverse phase HPLC: ¹H NMR (DMSO-*d*₆) δ 8.70 (s, 1 H), 8.41 (s, 1 H), 7.62 (s, 2 H), 5.89 (d, *J* = 7.25 Hz, 1 H), 4.53 (m, 1 H), 4.27 (s, 1 H), 4.08 (d, *J* = 3.6 Hz, 1 H), 2.29 (d, *J* = 6.4 Hz, 2 H), 2.15–1.99 (m, 1 H), 1.92–1.76 (m, 4 H), 1.52–1.38 (m, 1 H), 1.38–1.19 (m, 2 H), 1.02 (t, *J* = 6.3 Hz 3 H); ¹³C NMR (DMSO-*d*₆) 176.7, 169.2, 155.6,

148.9, 145.2, 141.6, 119.0, 87.7, 85.0, 84.6, 81.6, 73.1, 71.9, 43.2, 35.9, 33.3, 31.2, 28.3, 25.6, 15.0; HRMS (FAB) m/z 474.2196 [(M + H)⁺ calcd for C₂₂H₂₉N₆O₆ 474.2182].

4-{3-[6-Amino-9-(5-ethylcarbamoyl-3,4-dihydroxytetrahydrofuran-2-yl)-9H-purin-2-yl]prop-2-ynyl}-cyclohexanecarboxylic Acid Methyl Ester (110). The reaction of **89** with 2-iodo-NECA under the general conditions described above gave **110** (74 mg, 60%) as a white solid: ¹H NMR (CD₃OD) δ 8.23 (s, 1 H), 5.92 (d, J = 7.7 Hz, 1 H), 4.69–4.65 (dd, J = 7.7 Hz, 4.6 Hz, 1 H), 4.40 (s, 1 H), 4.24 (d, J = 4.6 Hz, 1 H), 3.59 (s, 3 H), 3.49–3.31 (m, 2 H), 2.31 (d, J = 6.6 Hz, 2 H), 2.10–2.09 (m, 1 H), 2.01–1.89 (m, 4 H), 1.61–1.32 (m, 5 H), 1.13 (t, J = 7.3 Hz, 3 H); ¹³C NMR (CD₃OD) δ 177.1, 171.1, 156.3, 149.3, 146.7, 142.4, 119.7, 89.6, 86.0, 85.5, 81.6, 74.0, 72.2, 51.2, 43.2, 36.8, 34.2, 31.8, 28.9, 26.2, 14.4; HRMS (FAB) m/z 487.2325 [(M + H)⁺ calcd for C₂₃H₃₁N₆O₆ 487.2305].

Acetic Acid 4-{3-[6-Amino-9-(5-ethylcarbamoyl-3,4-dihydroxytetrahydrofuran-2-yl)-9H-purin-2-yl]prop-2-ynyl}-cyclohexylmethyl Ester (111). The reaction of **87** with 2-iodo-NECA under the general conditions described above gave **111** (78 mg, 62%) as a white solid: ¹H NMR (CD₃OD) δ 8.22 (s, 1 H), 5.92 (d, J = 8.1 Hz, 1 H), 4.70–4.66 (dd, J = 8.1 Hz, 4.6 Hz, 1 H), 4.40 (d, J = 1.2 Hz, 1 H), 4.25–4.23 (dd, J = 4.6 Hz, 1.2 Hz, 1 H), 3.83 (d, J = 6.5, 2 H), 3.53–3.31 (m, 2 H), 2.29 (d, J = 6.5 Hz, 2 H), 1.97 (s, 3 H), 1.93–1.89 (m, 2 H), 1.79–1.75 (m, 2 H), 1.64–1.42 (m, 2 H), 1.12 (t, J = 7.3 Hz, 3 H), 1.09–0.91 (m, 4 H); ¹³C NMR (CD₃OD) δ 172.0, 171.2, 156.2, 149.3, 146.7, 142.5, 119.7, 89.6, 86.3, 85.5, 81.5, 74.0, 72.2, 69.6, 37.4, 37.2, 34.2, 32.1, 29.4, 26.4, 19.9, 14.5; HRMS (FAB) m/z 501.2469 [(M + H)⁺ calcd for C₂₄H₃₃N₆O₆ 501.2462].

5-{6-Amino-2-[3-(4-hydroxymethylcyclohexyl)prop-1-ynyl]purin-9-yl}-3,4-dihydroxytetrahydrofuran-2-carboxylic Acid Ethylamide (112). The reaction of **86** (30 mg, 0.2 mmol) with 2-iodo-NECA (28 mg, 0.07 mmol) under the general conditions described above gave **112** (7 mg, 24%) as a white solid: ¹H NMR (CD₃OD) δ 8.22 (s, 1 H), 5.92 (d, J = 7.7 Hz, 1 H), 4.70–4.66 (dd, J = 7.7 Hz, 4.8 Hz, 1 H), 4.40 (d, J = 1.2 Hz, 1 H), 4.25–4.23 (dd, J = 4.8 Hz, 1.2 Hz, 1 H), 3.51–3.37 (m, 2 H), 3.31 (d, J = 6 Hz, 2 H), 2.30 (d, J = 6.8 Hz, 2 H), 1.94–1.89 (m, 2 H), 1.83–1.78 (m, 2 H), 1.64–1.42 (m, 2 H), 1.12 (t, J = 7.3 Hz, 3 H), 1.09–0.91 (m, 4 H); ¹³C NMR (CD₃OD) δ 170.3, 155.4, 148.5, 146.0, 141.6, 118.8, 88.7, 85.5, 84.6, 80.6, 73.1, 71.3, 66.8, 39.6, 36.9, 33.3, 31.5, 28.6, 25.6, 13.5; HRMS (FAB) m/z 459.2373 [(M + H)⁺ calcd for C₂₂H₃₁N₆O₅ 459.2356].

Molecular Modeling and CoMFA Calculations. CoMFA values, using default parameters except where noted, were calculated through the QSAR option of SYBYL 6.5 on a silicon graphics Octane computer. The CoMFA grid spacing was 2.0 Å in the x , y , and z directions, and the grid region was automatically generated by the CoMFA routine to encompass all molecules with an extension of 4.0 Å in each direction. A sp³ carbon (for sterics) and a charge of +1.0 (for electrostatics) were used as probes to generate the interaction energies at each lattice point. The default value of 30 kcal/mol was used as the maximum electrostatic and steric energy cutoff.

Normalization of Biological Data. NECA (**78**) was normalized to a value of 10 nM, and all others compounds were adjusted appropriately by dividing or multiplying the analogue's experimental IC₅₀ by the appropriate scaling factor. The same normalization protocol was done for both A₁ and A_{2A} receptor data.

Data Analysis. Statistical correlations were performed using Jandel Scientific Software. All equations and correlations were calculated through the use of linear regressions based on the normalized data using SigmaStat for Windows Version 1.0. The plots shown in Figures 1–4 were constructed using SigmaPlot version 1.02a to which the best-fit linear regression line was added.

Conformational Analysis. We obtained X-ray structures from the Cambridge Database for adenosine and NECA and used these as representative low-energy conformations. The X-ray structure of NECA was used as a core to construct all NECA derivatives **37–62**, **95–103**, and **109–112**. In a similar

fashion, adenosine was used as the core for construction of derivatives **1–36**, **63–77**, **90–94**, and **104–108**. The corresponding X-ray portion of each analogue was held constant using AGGREGATE and the added functional groups were energy-minimized with the Tripos force field,³³ without solvent, using default bond angles and distances while neglecting electrostatics. In this manner, we obtained the lowest-energy conformation for each compound in Tables 1 and 2. In cases where long alkyl chains with multiple conformations were possible, the extended chain conformation was chosen.

Charge Calculations. All applied Coulson charges were calculated using AM1 (MOPAC) within SYBYL. The atomic charges were calculated in the singlet state with net charge equal to zero, keyword NOINTER, and normal convergence without geometry optimization and applied to the corresponding minimized molecular structure.

Molecular Alignment. All conformations for each compound in the training set (Table 1) were aligned with the FIT routine within SYBYL without changing the low-energy conformation previously obtained. All compounds were rms fit by aligning each atom of the adenine ring of the analogue to that of adenosine.

Partial Least Squares (PLS) Regression Analysis. Cross-validated and non-cross-validated PLS analyses for A₁ and A_{2A} receptors were performed within the SYBYL/QSAR routine. Separate cross-validations of the dependent columns log(adenosine A₁ IC₅₀) and –log(adenosine A_{2A} IC₅₀) within the CoMFA columns were performed without column filtering. In an additional experiment, we also constructed a model that contained multiple independent variables (dipole moment and log(A₁ IC₅₀) while maintaining –log(A_{2A} IC₅₀) as the dependent variable). As an example of our method for obtaining the non-cross-validated results, the analysis for adenosine A_{2A} was scaled by the CoMFA standard deviation and generated an optimum number of components equal to 4 and r^2 = 0.541. PLS analysis with non-cross-validation, performed with 4 components and 2.0 kcal/mol column filtering, resulted in dropping 2886 of 3146 columns and gave a standard error of estimate of 0.364, with a probability of r^2 = 0 (n_1 = 4, n_2 = 70) equal to 0.000, an F value of 78.242, and a final r^2 = 0.817. The relative steric 0.520 and electrostatic 0.480 contributions to the adenosine A_{2A} model were contoured as the standard deviation multiplied by the coefficient at 80% for favored steric (contoured in green) and favored positive electrostatic (contoured in blue) effects and at 20% for disfavored steric contoured in yellow and favored negative electrostatic (contoured in red) effects, as shown in Figure 5. In a similar manner, we derived a CoMFA model using adenosine A₁ IC₅₀ as well as adenosine A₁ IC₅₀/dipole as descriptors. We ultimately used the model generated from the adenosine A₁ IC₅₀/dipole descriptors, and the resulting CoMFA electrostatic and steric maps are shown in Figure 6. Using the appropriate CoMFA model and PREDICT PROPERTY in the QSAR module of SYBYL, we predicted adenosine A₁ and A_{2A} IC₅₀s using the appropriate model for compounds **90–113**.

Receptor Binding Data. Cortex and striatum were dissected from rats brain. They were rinsed with phosphate-buffered saline, pH 7.4. There were then homogenized in HE buffer (10 mM Na-HEPES, pH 7.4, 1 mM EDTA), plus a mixture of protease inhibitors (100 μ M PMSF, 100 μ M benzamidin, 2 μ M leupeptin, 2 μ M pepstatin A, 2 μ M aprotinin) and centrifuged at 20000g for 20 min. Pellets were resuspended and washed twice in the HE buffer plus protease inhibitors. Finally, the pellet was resuspended in the same buffer plus 10% sucrose and frozen until use.

For radioligand binding, striatum and cortex membranes were diluted to 25 μ g/50 μ L of striatum or 40 μ g/50 μ L of cortex and aliquoted in triplicate. Membranes were incubated with 5 mM Mg, 1 unit/mL adenosine deaminase and either 0.5 nM [¹²⁵I]APE (striatum) or [¹²⁵I]ABA (cortex) and increasing concentrations of competing agonist or antagonist for 3 h at room temperature. Tubes were filtered using a Brandel harvester and counted for 1 min in a gamma counter.

Abbreviations: CGS 21680, 2-[[4-(2-carboxyethyl)phenyl]-

ethylamino]-5'-N-ethylcarbamoyl-adenosine; CPA, N⁶-cyclopentyladenosine; DMSO, dimethyl sulfoxide; [¹²⁵I]ABA, 2-[2-(4-amino-3-[¹²⁵I]iodophenyl)ethylamino]adenosine; [¹²⁵I]APE, [¹²⁵I]-aminobenzyladenosine; NECA (5'-N-ethylcarboxamidoadenosine); PPh₃, triphenylphosphine; SAR, structure-activity relationship; TBAF, tetrabutylammonium fluoride.

Acknowledgment. This research was made possible by the University of Virginia Department of Chemistry as well as through funding provided by RO1 HL37942. M.L.B. thanks the UNCF/Merck Science Institute for funding support. We also thank The University of Nebraska Center for Mass Spectrometry for performing the HRMS analyses. Further appreciation is extended to Christine Dieckhaus for LC/MS work and Melissa Marshall for expert technical assistance with the receptor binding assays.

Supporting Information Available: Tables summarizing the predicted, actual, and residual values for the training and test sets as well as details on the PLS analyses. This material is available free of charge via the Internet at <http://pubs.acs.org>.

References

- (1) Muller, C. E.; Scior, T. Adenosine Receptors and Their Modulators. *Pharm. Acta Helv.* **1993**, *68*, 77–111.
- (2) Ralevic, V.; Burnstock, G. Receptors for Purines and Pyrimidines. *Pharmacol. Rev.* **1998**, *50*, 413–492.
- (3) DeNinno, M. P. Adenosine. *Annu. Rep. Med. Chem.* **1998**, *33*, 111–121.
- (4) Mubagwa, K.; Mullane, K.; Flameng, W. Role of Adenosine in the Heart and Circulation. *Cardiovasc. Res.* **1996**, *32*, 797–813.
- (5) Okusa, M. D.; Linden, J.; Macdonald, T.; Huang, L. Selective A_{2A} adenosine receptor activation reduces ischemia-reperfusion injury in rat kidney. *AJP: Renal* **1999**, *277*, F404–F412.
- (6) Cronstein, B. N. Adenosine, an Endogenous antiinflammatory agent. *J. Appl. Physiol.* **1994**, *76*, 5–13.
- (7) Grondin, R.; Bedard, P. J.; Tahar, A. H.; Bregoire, L.; Mori, A.; Kase, H. Antiparkinsonian effect of a new selective adenosine A_{2A} receptor antagonist in MPTP-treated monkeys. *Neurology* **1999**, *52*, 1673–1677.
- (8) Dixon, D. A.; Fenix, L. A.; Kim, D. M.; Raffa, R. B. Indirect Modulation of Dopamine D2 Receptors as Potential Pharmacotherapy for Schizophrenia: I. Adenosine Agonists. *Ann. Pharmacol.* **1999**, *33*, 480–488.
- (9) McPherson, J. A.; Bishop, G. G.; Sanders, J. M.; Rieger, J. M.; Heselbacher, S. E.; Gimple, L. W.; Powers, E. R.; Macdonald, T.; Sullivan, G.; Linden, J.; Sarembock, I. J. Adenosine A_{2A} Receptor Stimulation Reduces Inflammation and Neointimal Growth in a Murine Carotid Ligation Model. *Circulation*, submitted.
- (10) Cristalli, G.; Camaioni, E.; Vittori, S.; Volpini, R.; Borea, P. A.; Conti, A.; Dionisotti, S.; Ongini, E.; Monopoli, A. 2-Aralkynyl and 2-Heteroalkynyl derivatives of Adenosine-5'-N-ethyluronamide as Selective A_{2A} Adenosine Receptor Agonists. *J. Med. Chem.* **1995**, *38*, 1462–1472.
- (11) Daly, J. W.; Padgett, W. L.; Secunda, S. I.; Thompson, R. D.; Olsson, R. A. Structure-Activity relationships for 2-substituted Adenosines at A₁ and A₂ Adenosine Receptors. *Pharmacology* **1993**, *46*, 91–100.
- (12) Abiru, T.; Miyashita, T.; Watanabe, Y.; Yamaguchi, T.; Machida, H.; Matsuda, A. Nucleosides and Nucleotides. 107. 2-(Cycloalkylalkynyl)adenosines: Adenosine A₂ Receptor Agonists with Potent Antihypertensive Effects. *J. Med. Chem.* **1992**, *35*, 2253–2260.
- (13) Vittori, Z.; Camaioni, E.; Di Francesco, E.; Volpini, R.; Monopoli, A.; Dionisotti, S.; Ongini, E.; Cristalli, G. 2-Alkenyl and 2-Alky Derivatives of Adenosine and Adenosine-5'-N-Ethyluronamide: Different Affinity and Selectivity of E- and Z-Diastereomers at A_{2A} Adenosine Receptors. *J. Med. Chem.* **1996**, *39*, 4211–4217.
- (14) Camaioni, E.; Di Francesco, E.; Vittori, S.; Volpini, R.; Cristalli, G. Adenosine Receptor Agonists: Synthesis and Biological Evaluation of the Diastereomers of 2-(3-Hydroxy-3-phenyl-1-propyn-1-yl)NECA. *Bioorg. Med. Chem.* **1997**, *5*, 2267–2275.
- (15) Hutchinson, A. J.; Williams, M.; de Jesus, R.; Yokoyama, R.; Oei, H. H.; Ghai, G. R.; Webb, R. L.; Zoganas, H. C.; Stone, G. A.; Jarvis, M. F. 2-(Arylalkylamino)adenosin-5'-uronamides: A new Class of Highly Selective Adenosine A₂ Receptor Ligands. *J. Med. Chem.* **1990**, *33*, 1919–1924.
- (16) Matsuda, A.; Shinozaki, M.; Yamaguchi, T.; Homma, H.; Nomoto, R.; Miyasaka, T.; Watanabe, Y.; Abiru, T. Nucleosides and Nucleotides. 103. 2-Alkynyladenosines: A Novel Class of Selective Adenosine A₂ Receptor Agonists with Potent Antihypertensive Effects. *J. Med. Chem.* **1992**, *35*, 241–252.
- (17) Cristalli, G.; Eleuteri, A.; Vittori, S.; Volpini, R.; Lohse, M. J.; Klotz, K. 2-Alkynyl Derivatives of Adenosine and Adenosine-5'-N-ethyluronamide as Selective Agonists at A₂ Adenosine Receptors. *J. Med. Chem.* **1992**, *35*, 2363–2368.
- (18) Graaf, P. H. V.; Nilsson, J.; Schaick, E. A. V.; Danhof, M. Multivariate Quantitative Structure-Pharmacokinetic Relationships (QSPKR) Analysis of Adenosine A₁ Receptor Agonists in Rat. *J. Pharm. Sci.* **1999**, *88*, 306–312.
- (19) Baraldi, P. G.; Borea, P. A.; Bergonzoni, M.; Cacciari, B.; Ongini, E.; Recanatini, M.; Spaluto, G. Comparative Molecular Field Analysis (CoMFA) of a Series of Selective Adenosine Receptor A_{2A} Antagonists. *Drug Dev. Res.* **1999**, *46*, 126–133.
- (20) Moro, S.; Li, A.; Jacobsen, K. Molecular Modeling Studies of Human A₃ Adenosine Antagonists: Structural Homology and Receptor Docking. *J. Chem. Inf. Comput. Sci.* **1998**, *38*, 1239–1248.
- (21) Li, A.; Moro, S.; Forsyth, N.; Melman, N.; Ji, X.; Jacobson, K. A. Synthesis, CoMFA Analysis, and Receptor Docking of 3,5-Diacetyl-2,4-Dialkylpyridine Derivatives as Selective A₃ Adenosine Receptor Antagonists. *J. Med. Chem.* **1999**, *42*, 706–721.
- (22) Moro, S.; van Rhee, A. M.; Sanders, L. H.; Jacobson, K. A. Flavonoid Derivatives as Adenosine Receptor Antagonists: A Comparison of the Hypothetical Receptor Binding Site Based on a Comparative Molecular Field Analysis Model. *J. Med. Chem.* **1998**, *41*, 46–52.
- (23) Li, A.; Moro, S.; Melman, N.; Ji, X.; Jacobson, K. A. Structure-Activity Relationships and Molecular Modeling of 3,5-Diacetyl-2,4-dialkylpyridine Derivatives as Selective A₃ Adenosine Receptor Antagonists. *J. Med. Chem.* **1998**, *41*, 3186–3201.
- (24) Siddiqi, S. M.; Pearlstein, R. A.; Sanders, L. H.; Jacobson, K. A. Comparative Molecular Field Analysis of Selective A₃ Adenosine Receptor Agonists. *Bioorg. Med. Chem.* **1995**, *3*, 1331–1343.
- (25) McDougal, P. G.; Rico, J. G.; Oh, Y.; Condon, B. D. A Convenient Procedure for the Monosilylation of Symmetric 1,n-Diols. *J. Org. Chem.* **1986**, *51*, 3388–3390.
- (26) Kabalka, G. W.; Varma, M.; Varma, R. S. Tosylation of Alcohols. *J. Org. Chem.* **1986**, *52*, 2486–2488.
- (27) Manchand, P. S.; Schwartz, A.; Wolff, S.; Belica, P. S.; Madan, P.; Patel, P.; Saposnik, S. J. Synthesis of an Orally Active PAF Antagonist of the N-[4-(3-Pyridinyl)butyl]pentadecanamide Class. *Heterocycles* **1993**, *35*, 1350–1369.
- (28) Luthin, D. R.; Olsson, R. A.; Thompson, R. D.; Sawmiller, D. R.; Linden, J. Characterization of Two Affinity States of Adenosine A_{2A} Receptors with a New Radioligand, 2-[2-(4-amino-3-[¹²⁵I]iodophenyl)ethylamino]adenosine. *Mol. Pharmacol.* **1995**, *47*, 307.
- (29) Linden, J.; Patel, A.; Sadek, S. [¹²⁵I]aminobenzyladenosine, a New Radioligand with Improved Specific Binding to Adenosine Receptors in Heart. *Circ. Res.* **1985**, *56*, 279.
- (30) Klooster, W. T.; Ruble, J. R.; Craven, B. M.; McMullan, R. K. *Acta Crystallogr., Sect. B* **1991**, *47*, 376.
- (31) Moos, W. H.; Hamilton, H. W.; Ortwein, D. F.; Taylor, M. D.; McPhail, A. T. *Nucleosides Nucleotides* **1989**, *8*, 449.
- (32) Still, W. C.; Kahn, M.; Mitra, A. Rapid Chromatographic Technique for Preparative Separations With Moderate Resolution. *J. Org. Chem.* **1978**, *43*, 2923–2925.
- (33) Clark, M. D.; Cramer, R. D., III; Opdenbosch, N. V. *J. Comput. Chem.* **1989**, *10*.

JM0003642